Power Law Behavior in Protein Desorption Kinetics Originating from Sequential Binding and Unbinding

Megan J. Armstrong^{†1}, Juan B. Rodriguez III^{†1}, Peter Dahl², Peter Salamon², Henry Hess^{1*}, Parag Katira^{2*}

- ¹ Columbia University, New York, NY 10027, United States
- ² San Diego State University, San Diego, CA 98182, United States
- * corresponding authors: hhess@columbia.edu, pkatira@sdsu.edu
- † indicates equal contribution

ABSTRACT

The study of protein adsorption at the single molecule level has recently revealed that the adsorption is reversible, but with a long-tailed residence time distribution which can be approximated with a sum of exponential functions putatively related to distinct adsorption sites. Here it is proposed that the shape of the residence time distribution results from an adsorption process with sequential and reversible steps that contribute to overall binding strength resembling "zippering". In this model, the survival function of the residence time distribution of single proteins varies from an exponential distribution for a single adsorption step to a power law distribution with exponent -½ for a large number of adsorption steps. The adsorption of fluorescently labeled fibrinogen to glass surfaces is experimentally studied with single molecule imaging. The experimental residence time distribution can be readily fit by the proposed model. This demonstrates that the observed long residence times can arise from stepwise adsorption rather than rare but strong binding sites and provides guidance for the control of protein adsorption to biomaterials.

INTRODUCTION

The interactions of proteins with surfaces have implications in biocompatibility of a surface,¹⁻⁴ protein separation,⁵⁻⁹ and pharmaceutical nanoparticle development.¹⁰ Protein adsorption affects the ability of both the protein and the surface to fulfill their intended purpose in these capacities.¹¹ Protein adsorption can be quantitatively studied by a variety of techniques¹²⁻¹⁸ and the data are typically interpreted as having Langmuir-type adsorption kinetics composed of a constant signal from an irreversibly adsorbed protein fraction and exponential desorption kinetics from a reversibly bound protein fraction.^{11,19-24}

Recent advances in single molecule microscopy have enabled the observation of individual protein-surface interaction events.^{25–27} Protein adsorption studies at the single molecule level have shown that the amount of time proteins of a given type are bound to the surface is broadly distributed and well-approximated by the sum of several exponential functions.^{8,28} The determined desorption rate constants are thought to reflect distinct surface sites,²⁹ distinct subpopulations of adsorbing proteins,²⁸ or transitions between different binding states (stepwise denaturation).³⁰ However, an assignment of each rate to a specific type of event is usually not attempted.^{28,31}

In the field of economics, Benoit Mandelbrot has sharply criticized the fitting of various data with sums of exponentials on the grounds that the data can often be concisely fit with power

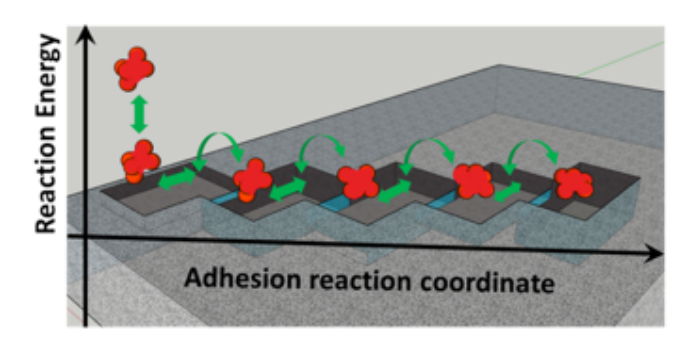
laws to which the sum of exponentials often provide only awkward approximations relying on many additional parameters.³² However, it is often practical from a computational perspective to approximate a power law distribution with a sum of exponentials, and an approach to find the optimal number of exponentials is defined in the literature.³³

This raises the question if the same arguments apply to the interpretation of single molecule data. The "sum of exponentials vs. power laws" debate however is not simply about the search for the model which best satisfies an information criterion, 34,35 but about which mechanistic interpretation is appropriate. A number of physical mechanisms giving rise to power laws have been reviewed by Newman. 36

Here, we propose that the observed protein desorption kinetics originates from the sequential and reversible establishment of protein-surface contacts, where each contact adds a small contribution to the overall binding energy (Fig. 1). After making the initial contact, the protein performs a slightly biased random walk over a large number of small energy barriers until it makes a maximum number of contacts. This mechanism corresponds to the "statistical zippering" observed by Penna et al. in molecular simulations of peptide adsorption.³⁷ In contrast to the desorption kinetics arising from the passage over a single, dominant energy barrier (exponentially distributed residence times), the unbiased one-dimensional random walk

along the reaction coordinate results in a power law with exponent -1/2 for the cumulative residence time distribution for an infinite number of barriers (Fig. 2a).

We first describe the theoretical model and how it is fit to experimental data, and then present measurements of the residence time distributions of fluorescently labeled fibrinogen (Fg) on glass surfaces. The experimental data are comparable to previously published data of fibrinogen adsorption to fused silica and other surfaces by the Schwartz and Landes groups^{8,28,38–41}. We interpret the data using the statistical zippering model and discuss the implications.



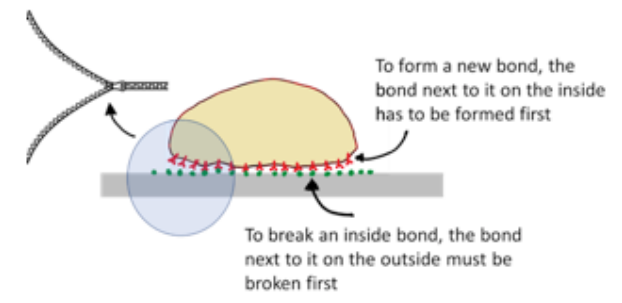


Figure 1. The protein adsorption process as sequential transitions from one energy conformation to another. The separate reaction coordinates of the individual transitions ensure sequential transitions as the protein binds to and unbinds from a surface.

THEORY

It is well known that proteins undergo conformational changes as they interact and adhere to surfaces. Here we assume that these conformational changes occur in a sequential manner, where each particular conformational change can only occur if a previous conformational change has been achieved. Each of these changes are reversible, but the reversal is only possible to the immediately preceding conformation of the protein on the surface. This process can be seen schematically in Figure 1. In other words, during adsorption the protein traverses a multidimensional binding energy surface along a preferred path featuring distinct binding states connected via low barriers.

We also assume that there is a certain maximum number of states in this reversible adsorption process, beyond which it is impossible to further change the structure of the protein without irreversibly denaturing it. The process of protein adsorption to a surface can then be approximated by a 1D random walk along the various conformations with a reflecting barrier at the end. A protein interacting with the surface starts at the first conformation with a single attachment and follows a sequence of conformational changes along this path. The protein can desorb from the surface when it returns back to the initial conformation. The residence time of a protein on a surface is

then given by the time it takes for the protein starting in the initial attached position to leave the surface. If there is an infinite number of distinct binding states (no reflecting boundary), the residence time distribution is given by the inverse Gaussian distribution.⁴³ If the random walk along the chain of conformational changes is unbiased, this becomes the Levy distribution which has a power law tail with an exponent of -0.5. However, the presence of a reflective barrier makes it difficult to obtain a closed form expression for the residence time distributions and instead we simulate the process with the following algorithm that follows the Gillespie formulation⁴⁴:

- i. The simulation initiates with a protein attached to the surface in an initial conformation (Conformational State 1).
- ii. In accordance with the Gillespie algorithm, the time step, t is drawn from an exponential distribution whose average is the timescale τ of transitions between protein states⁴⁴ (eq. 24a in ⁴⁴).
- iii. The protein undergoes a change to the previous attached conformation at the next timestep with probability p or a new conformation with the probability 1-p⁴⁴ (eq. 24b in ⁴⁴).
- iv. Repeat (ii) and (iii) until the protein leaves the surface (the state prior to the initial bound configuration) or reaches the maximum conformationally changed bound state (N), at which point it can only go to the previous conformation (p=1).

Using this simple simulation process, we can generate the residence time distributions for proteins interacting with a surface. We can also fit the results of this simulation to experimental data with the following three fit parameters – 1) the timescale $(\tau),\ 2)$ p or 1-p (for each of the conformational states), and 3) the maximum number of conformational states possible (N). The timescale reflects the kinetics of the process – how slow or fast the transitions are. The transition probabilities reflect the height difference in the energy barriers to the next or the previous neighboring conformations. The maximum number of conformational changes allowed provides the time to most strongly adhered state.

The model parameters p, 1-p, and τ can be related to other chemical reaction kinetics determining parameters. For example, $\frac{p}{\tau}=k_-$ is the backward reaction rate, $\frac{1-p}{\tau}=k_+$ is the forward reaction rate (first order approximation in τ), and $k_BT \ln((1-p)/p)=\Delta E$ is the difference in the energy barrier heights for forward and backwards transitions. However, here we stick to the use of p and τ as the model parameters because the discussion seems more linear in terms of adsorption/desorption bias and process time scales.

For a protein with a footprint of about $50~\text{nm}^2$, such as BSA, 45 hundreds of distinct contacts between the atoms on the surface and the atoms and functional groups of the protein could be established. However, the pathway to complete binding could be dominated by the activation energies between a relatively small number of large conformational rearrangements which permit new contacts between groups of atoms on the surface and on the protein. Each contact may contribute significantly less than one k_BT to the overall binding energy as a net result of multiple weak intermolecular interactions. However, the activation energies for transition between states require the establishment of new surface contacts as well as internal rearrangements of the protein conformation and can be on the order of $20\text{-}30~k_BT$. With a frequency factor on the order of 10^{10}

 s^{-1} , this would imply timescales for the transitions on the order of milliseconds to seconds.

The probability p (and consequently 1-p) can vary between conformational states, however we find that if the forward and backward transition probabilities across all states are similar, the process can be approximated by a single average forward and backward transition probability (Figure S1). p=0.5 implies no bias between transitioning to the next bound conformation vs the previous conformation, while p>0.5 implies a bias towards previous more lightly bound conformations and the unbound state. On the other hand, p<0.5 implies a bias towards the more strongly bound and maximally bound conformations. Similarly, a protein may traverse a different reaction pathway where the sequence of accessed states is altered (e.g. if the proteins first binds in a different state). If the energy levels between the states are similar, this again can be approximated by a single average forward and backward transition probability.

The effect of these three parameters on simulated protein residence times can be seen in Figure 2a-c. As mentioned above, an unrestricted random walk (with infinite sequential conformations) results in a power law distribution at no or slight bias. However, if the bias towards the unbound state is higher, then even for an unrestricted random walk, the power phase quickly merges with an exponential tail. In scenarios where the protein has a limited number of conformational changes, the power law residence time distribution for short residence times has again an exponential tail for long residence times. A smaller maximum number of conformational changes or a faster transition to the strongly bound states, reduces the length of the power law portion of the residence time distribution and merges it more quickly into an exponential distribution. The bias of the random walk also alters the exponent of the power law portion of the residence time distribution. The time scale of the transitions between the conformational changes does not alter the exponent of the power law regime but speeds up the transition to the exponential regime and the decay rate of the exponential regime.

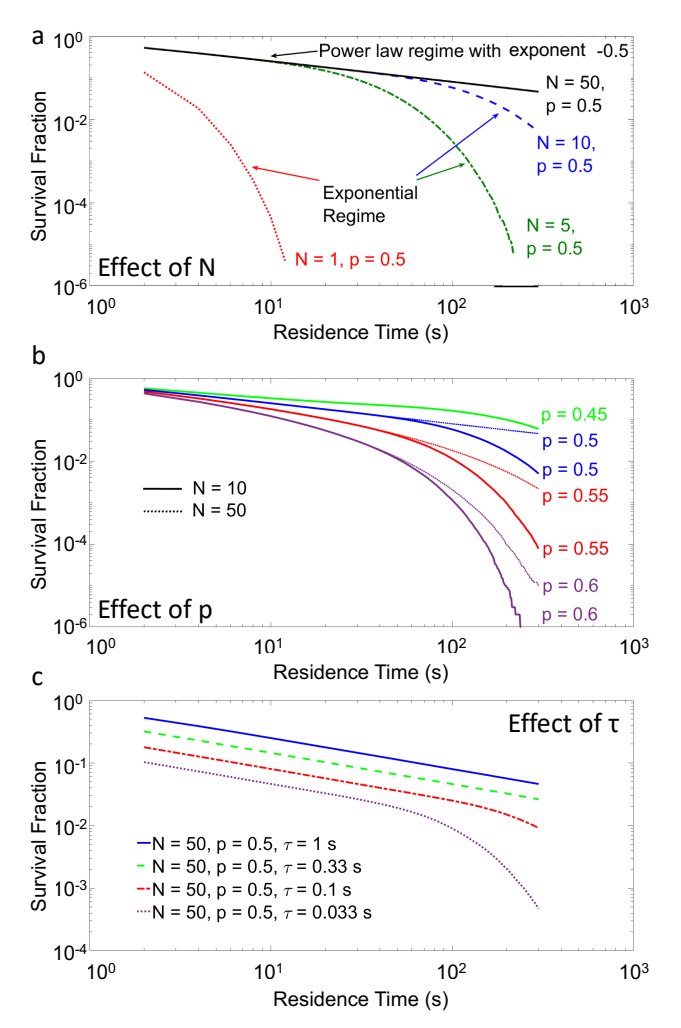


Figure 2. Simulated residence time distribution of proteins on surfaces. The effect of the three model parameters is shown in (a) for N, maximum number of conformational states the protein can achieve; in (b) for p, the likelihood of transitioning to the previous conformational state (indicates bias in the adsorption/desorption process); and in (c) for τ , the average timescale for transitions between two neighboring conformation states.

EXPERIMENTAL SECTION

Single Molecule Imaging. Fibrinogen (Fg) conjugated with AlexaFluor 488 from Thermo Fisher Scientific (F13191, Lot 1904433, labeling ratio: 9) was reconstituted in 10 mM phosphate buffered saline (PBS) at 1 mg/mL, stored at 4° C and used without further purification.

Flow cells were constructed from cleaned glass coverslips (#1 thickness, VWR Inc.), cleaned by sonicating in ultrapure water ($\geq 18~M\Omega\text{-cm}$), acetone, and 1M potassium hydroxide for 20 minutes each and rinsing three times after each step with ultrapure water. After drying at 40°C, the coverslips were plasma-cleaned in a UV-ozone cleaner before a final 20-minute sonication in ultrapure water. Coverslips were then dried again at 40°C and stored in sealed glass jars for less than 24 hours before use. Flow cells were assembled by taping a 22x22 mm coverslip to a 24x60 mm coverslip with two strips of double-sided tape in order to create a 5-10 mm wide channel between the strips of tape.

Fg (45 pM) solutions were prepared from the stock solution for each experiment by serial dilutions in 10 mM PBS at pH 7.4 with 100 mM DL-dithiothreitol (Sigma-Aldrich D0632; to reduce photobleaching) and filled into the flow cells by capillary action. The cells were sealed with vacuum grease to prevent evaporation.

Images were acquired with an epi-fluorescence microscope (Ti-Eclipse, Nikon Inc.) with a TIRF module using a 100x 1.45 NA oil objective and a back-illuminated EMCCD camera (Andor iXon). Samples were illuminated during the exposure time only with a 488 nm diode laser (LuxX, Omicron Laserprodukte GmbH) with 12 mW laser power. Images were acquired in 100 ms exposures with 1 s between the start of each frame for 30 minutes. The time between exposures minimizes the appearance of photoblinking as it allows the fluorophore to recover out of the dark triplet state. The electron multiplier gain was set to 150. The pixel noise level (S.D. of the dimmest 95% of all pixels in the flattened images) was 4 counts. The photobleaching rate is (1500 s)-1 as determined from the intensity changes of spots present throughout the observation window. At a labeling ratio of 9, this means that for a fibringen molecule with the average 9 labels the probability that at least one fluorophore remains active after 1000 s (the largest observed residence time) is larger than 99.8%. Even a fibrinogen molecule with only 3 labels initially has an almost 90% chance of retaining an active fluorophore after 1000 s.

Single Molecule Identification and Tracking. Videos of protein solutions were analyzed using ImageJ by visually identifying bright spots in each frame. For each spot, the frames at which the spot appears and disappears was recorded to calculate the residence time. Also recorded are spots present in the first frame and spots present in the last frame. Intensities values for each particle are calculated by summing the intensity of a 5 pixel-wide diamond after subtracting the median intensity of the 3 pixel corners of a 5 pixel-wide square from each pixel. Large spots and spots with close neighbors can be assigned negative intensities. The camera noise of 4 counts in each pixel gives rise to an intensity noise of 15 counts in each analyzed spot.

Survival Analysis. The probability that a protein has a surface lifetime of t or longer was determined by estimating the survival function, S(t). The measured residence times were used to construct an empirical cumulative distribution function and the complementary survival function using the Kaplan-Meier method as described in detail elsewhere⁴⁶ Briefly, the number of proteins with each given lifetime was normalized by the number of proteins with that lifetime or longer. The normalization includes proteins who are still present in the last frame. The normalized count of proteins with each lifetime were aggregated into a cumulative distribution.

RESULTS AND DISCUSSION

The experimental results for Fibrinogen (Fn) adsorption to glass and their analysis are shown in Figure 3. At the chosen concentration of fibrinogen (45 pM), the bright spots arising from adsorbed fibrinogen are well separated on the surface (Fig. 3a). While automated tracking software identified up to 40,000 objects in the stack of images, we were unable to find a suitable compromise threshold value for object identification which did not return unacceptably large numbers of false positives or negatives. We thus visually identified bright spots and

manually recorded their appearance and disappearance, yielding only 187 new binding events during the 1,800 s observation window in addition to 1147 spots present initially (Fig. 3b). Uncensored (182 appear and disappear) and right-censored (5 appear and remain to the end) events were used to construct the survival function (also referred to as the cumulative residence time distribution) using the Kaplan-Meier method (Fig. 3c).

The cumulative residence time distribution, S(t), has the multiexponential appearance in a log-linear plot described by Kastantin et al.²⁸ and a maximum entropy fit⁴⁷ yields four exponential components $(S(t) = \sum_{i=1}^{n} A_i e^{-t/\theta_i}$, where n = 4, A = [0.6497, 0.3401, 0.5202, 0.08673] and θ = [0.7752, 15.26, 159.3, 1029]). The single-barrier model of protein adsorption predicts that the cumulative residence time distribution is fit by a single exponential (appearing as a line in a log-linear plot).48 Kastantin et al. proposed that the multi-exponential appearance arises from multiple aggregation states in the fibrinogen population that bind to the surface with distinct strength. The size of the fibrinogen aggregate is correlated with its brightness which enabled Kastantin et al. to identify the subpopulations with different residence times (varying from 0.6 s to 70 s) with the subpopulations with different brightness (varving ten-fold in intensity). Our attempts at automated tracking reproduced this behavior, including the shift of longer-lived objects towards higher intensities. However, our manual tracking procedure identified in average less bright objects with a narrower intensity distribution, which does not shift towards longer residence times if objects residing less than 100 s on the surface (70% of the sample) are excluded (Figure 3c, Figure S2). This suggests that the sample is composed of identical objects, likely fibrinogen monomers. This is further supported by the finding that subdividing our sample in four fractions of different intensities yields similar cumulative residence time distributions (Fig. 3c). The similarity of the residence time distribution for the four fractions of different initial intensities also lends support to the claim that the residence time distributions are not affected by photobleaching, since otherwise the initially dimmer fractions would disappear faster. Our central point here is that even a single population with respect to intensity delivered an apparently multi-exponential cumulative residence time distribution.

Fitting the sequential unbinding model described above yields an excellent fit to the cumulative residence time distribution with parameters p = 0.367, N = 4, τ = 6 s (Figure 3d, Figures S3, S4) lending support to the concept that the observed residence time distribution arises from the protein traversing a potential energy surface with sequential minima.

The experimental results obtained here match the big picture painted by the group of D. Schwartz^{9,28-31,38,39,41}: The cumulative residence time distributions appear multi-exponential with time constants from sub-seconds to minutes. The adsorption events are not uniformly distributed across the surface, but reveal a certain "patchiness" likely related to inhomogeneities in the surface. Differences in the specific values can be attributed to differences in the utilized surfaces and the analysis, but are not our focus here. Our focus is to answer the question if the multi-exponential appearance of the cumulative residence time distributions can be explained by the above introduced sequential desorption model.

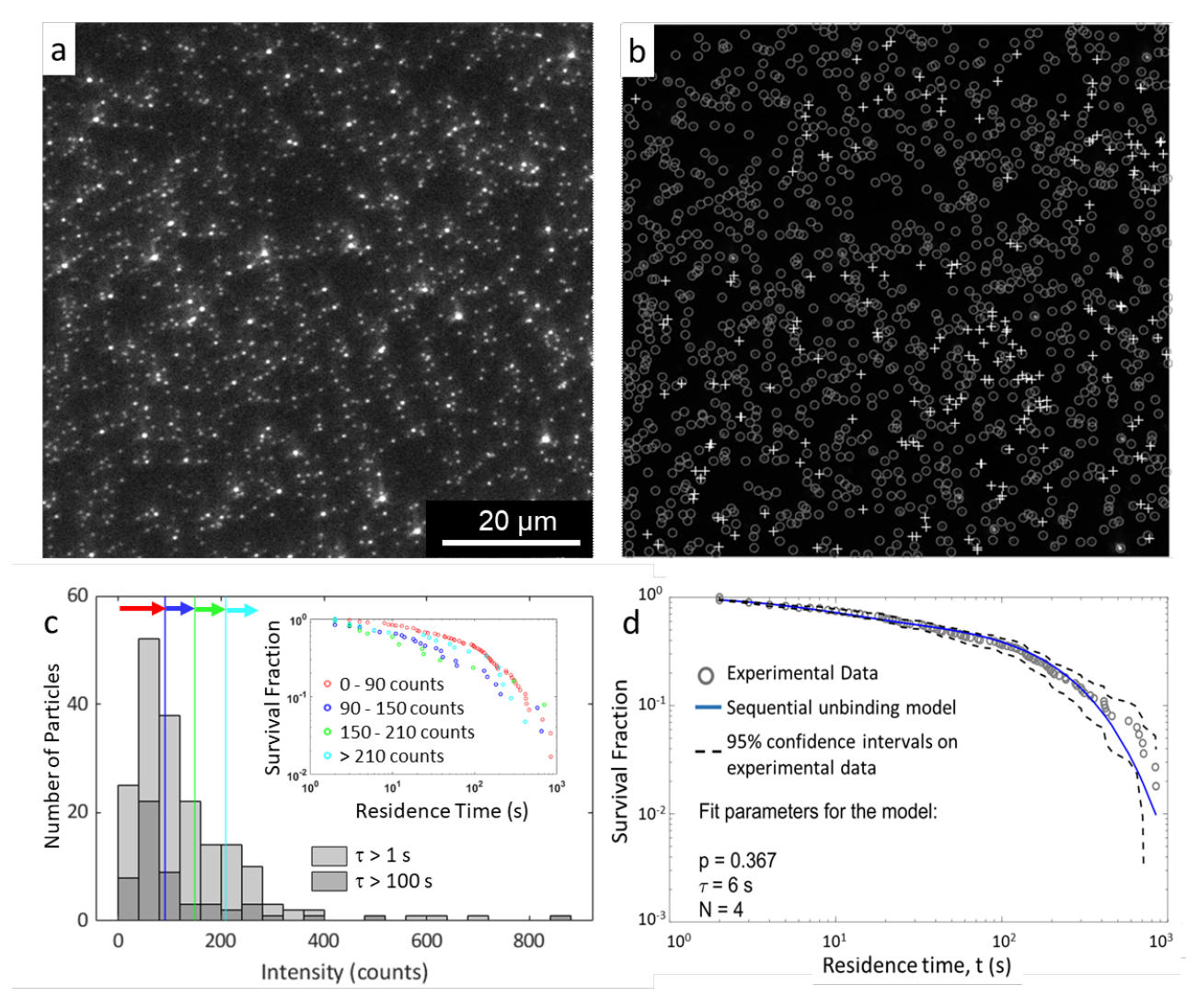


Figure 3. Adsorption of single fibrinogen molecules to a glass surface. (a) Representative fluorescence microscopy image. (b) Distribution of manually tracked spots (circles: initially present; crosses: appeared during the observation window). (c) Intensity distribution of all objects (187 with $\tau > 1$ s) and long-lived objects (54 with $\tau > 100$ s), inset: Survival fractions for populations separated by initial intensity. (d) Fit of the sequential unbinding model to the cumulative residence time distribution calculated from 187 binding events.

The sequential desorption model fits the observed cumulative residence time distribution well with only three parameters: the lifetime of the binding states τ , the probability to transition from one state towards the less strongly bound state p, and the number of distinct binding states N.

The fitted lifetime of the binding states of 6 s implies an activation energy on the order of 25 k_BT if we assume a frequency pre-factor of 10^{10} s⁻¹. The energy barrier from solution to the first adsorption state can be calculated by comparing the collision rate of fibrinogen with the surface given by $J = C[k_BT/(2\pi m)]^{1/2} = 5 \times 10^{16} m^{-2} s^{-1}$ according to Jung and Campbell⁴⁹ with the observed rate of adsorption of 187 molecules per field-of-view in the 1,800 s observation window, which yields a sticking probability of 3×10^{-10} and an activation energy of 22 k_BT. The large number of initially present adsorbed fibrinogens relative to the number of later adsorbing fibrinogens (Fig. 3b) indicates that the solution is likely significantly depleted of fibrinogen, which would lower the collision rate and increase the activation energy by a few k_BT. The rough

correspondence between the activation energies for the transition from the solution to the first binding state and the transitions between subsequent binding states is reassuring.

The fitted probability to transition to a less strongly bound state is 0.367, which corresponds to a difference in free energies between the states of $\Delta E = k_B T \ln \left((1-p)/p \right) = 0.5 k_B T$. This small energy difference between adjacent energy barriers is critical for the reversibility of the adsorption process, and is reasonable in the context of the exquisite balance between the various enthalpic and entropic contributions responsible for a conformational state of a protein.

The fit selects a number of 4 distinct binding states. It may be a stretch to relate these states to the adsorption of the four large peripheral domains of fibrinogen (PDB: 3GHG), but the states likely represent binding of larger domains and not the binding of individual amino acids, of which we expect hundreds to make contact with the surface.

Overall, the fit parameters are reasonable given the energy and time scales of protein adsorption. At the same time, the threeparameter model presents a stylized version of highly varied events reduced to their very essence. Of course, each protein traverses a slightly different potential energy surface on a path crossing energy barriers in different sequences (e.g. due to random starting points on the potential energy surface). The combination of these individual protein fates gives the appearance that fibrinogen molecules travel on a timescale of seconds between four sequential binding states with a slight bias towards stronger binding. Further experiments with different proteins are needed to correlate protein properties with the model parameters. However, from our perspective, the sequential adsorption mechanism as an explanation for the multi-exponential appearance of the cumulative lifetime distribution of a single species has the advantage that it does not require the identification of multiple adsorption sites whose binding strengths line up just as needed to approximate a power law.

From a broader perspective, the appearance of power law behavior – with its attendant emphasis on long tails and absence of averages⁵⁰ – in chemical systems is both disconcerting and tantalizing. Power law behavior related to the blinking of quantum dots has been extensively studied, and it has been demonstrated that power law behavior of individual objects and events can give rise to intriguing phenomena in ensembles, such as sub-diffusion, statistical aging and non-ergodicity.^{51,52} The connection between single molecule adsorption and the ensemble adsorption measurement¹² has not yet been studied in similar detail.

From the perspective of the research community studying protein adsorption, the present work can be considered to be a conceptual extension of earlier two state models.^{53,54} Advances in the mechanistic understanding of protein adsorption and the properties of protein and surface governing it will require further experimental studies of different combinations of protein, surface, and solution properties. 55,56 The present approach is focused on isolated proteins, which can limit its relevance to many practical situations.⁵⁷ It also requires fluorescent labeling of the proteins, altering their surface properties by introducing hydrophobic fluorophores in addition to the native hydrophobic patches.58,59 While fluorescently labeled proteins are a classic tool to study protein adsorption,60-62 recent work highlights the potential of the fluorophores to alter the adsorption kinetics. 63,64 Understanding protein adsorption remains a multifaceted challenge,65-67 and the contribution of the current work - similar to our earlier random sequential adsorption model of protein binding to non-fouling surfaces⁶⁸ - is to refocus the spotlight from the surface back onto the protein.

CONCLUSIONS

The multi-exponential appearance of the cumulative residence time distribution in single protein adsorption measurements is consistent with a sequential desorption model, where the protein reversibly transitions between distinct adsorption states in a biased random walk. In the case of fibrinogen adsorption experimentally studied here, the cumulative residence time distribution is best fit with 4 states, a transition time between states of 6 s, and a significant bias for transitions towards stronger binding. This mechanistic model of protein adsorption has potentially interesting consequences for bulk measurements.

ASSOCIATED CONTENT

Supporting Information

Survival functions for a 10-barrier landscape with small variations in transition probability. Inset of Figure 3c. Survival functions for a 4-barrier landscape with 6 s transition time and small variations in backward transition probability p around 0.367. Effect of changing the fit parameters near the optimal fit. The MATLAB simulation codes used to model and fit protein residence times based on the sequential adsorption process can be found at https://github.com/compact-matterlab/seq-protein adsorption.

AUTHOR INFORMATION

Corresponding Authors

Present Addresses

- Department of Biomedical Engineering, Columbia University, New York, NY 10027, USA
- Mechanical Engineering Department, San Diego State University, San Diego, CA 98182, USA
- Department of Mathematics and Statistics and Viral Information Institute, San Diego State University, San Diego, CA 92182, USA

Author Contributions

P.K., H.H., and M.J.A. conceived and designed the research. P.S. and P.K. conceptualized the sequential desorption model. P.D. and P.K. performed the simulations and fitting. M.J.A. and J.B.R. performed all the experiments. J.B.R. analyzed the experimental data. All the authors discussed the results and commented on the manuscript.

† indicates equal contribution

Notes

The authors declare no competing financial interests.

ACKNOWLEDGMENT

M.A. thanks the National Science Foundation for the Graduate Research Fellowship DGE 16-44869. Financial support under NSF grant NSF-DMR grant 1807514 is gratefully acknowledged by J.B.R. and H.H. Financial support under DoD ARO grant W911NF-17-1-0413 is gratefully acknowledged by P.K.

REFERENCES

- (1) Lynch, I.; Cedervall, T.; Lundqvist, M.; Cabaleiro-Lago, C.; Linse, S.; Dawson, K. A. The Nanoparticle-Protein Complex as a Biological Entity; a Complex Fluids and Surface Science Challenge for the 21st Century. *Adv. Colloid Interface Sci.* **2007**, *134–135*, 167–174. https://doi.org/10.1016/j.cis.2007.04.021.
- (2) Lynch, I.; Salvati, A.; Dawson, K. A. Protein-Nanoparticle Interactions: What Does the Cell See? *Nat. Nanotechnol.* **2009**, *4* (9), 546–547. https://doi.org/10.1038/nnano.2009.248.

- (3) Monopoli, M. P.; Walczyk, D.; Campbell, A.; Elia, G.; Lynch, I.; Baldelli Bombelli, F.; Dawson, K. A. Physical-Chemical Aspects of Protein Corona: Relevance to in Vitro and in Vivo Biological Impacts of Nanoparticles. J. Am. Chem. Soc. 2011, 133 (8), 2525–2534. https://doi.org/10.1021/ja107583h.
- (4) Monopoli, M. P.; Bombelli, F. B.; Dawson, K. A. Nanobiotechnology: Nanoparticle Coronas Take Shape. *Nat. Nanotechnol.* **2011**, *6* (1), 11–12. https://doi.org/10.1038/nnano.2011.267.
- (5) Kisley, L.; Landes, C. F. Molecular Approaches to Chromatography Using Single Molecule Spectroscopy. *Anal. Chem.* **2015**, *87* (1), 83–98. https://doi.org/10.1021/ac5039225.
- (6) Kisley, L.; Chen, J.; Mansur, A. P.; Dominguez-Medina, S.; Kulla, E.; Kang, M. K.; Shuang, B.; Kourentzi, K.; Poongavanam, M. V.; Dhamane, S.; Willson, R. C.; Landes, C. F. High Ionic Strength Narrows the Population of Sites Participating in Protein Ion-Exchange Adsorption: A Single-Molecule Study. J. Chromatogr. A 2014, 1343, 135–142. https://doi.org/10.1016/j.chroma.2014.03.075.
- (7) Kisley, L.; Chen, J.; Mansur, A. P.; Shuang, B.; Kourentzi, K.; Poongavanam, M.-V.; Chen, W.-H.; Dhamane, S.; Willson, R. C.; Landes, C. F. Unified Superresolution Experiments and Stochastic Theory Provide Mechanistic Insight into Protein Ion-Exchange Adsorptive Separations. *Proc. Natl. Acad. Sci.* **2014**, 111 (6), 2075–2080. https://doi.org/10.1073/pnas.1318405111.
- (8) Kisley, L.; Patil, U.; Dhamane, S.; Kourentzi, K.; Tauzin, L. J.; Willson, R. C.; Landes, C. F. Competitive Multicomponent Anion Exchange Adsorption of Proteins at the Single Molecule Level. *Analyst* 2017, 142 (17), 3127–3131. https://doi.org/10.1039/C7AN00701A.
- (9) Mabry, J. N.; Skaug, M. J.; Schwartz, D. K. Single-Molecule Insights into Retention at a Reversed-Phase Chromatographic Interface. *Anal. Chem.* 2014, 86 (19), 9451–9458. https://doi.org/10.1021/ac5026418.
- (10) Wertz, C. F.; Ryde, N. P. United States Patent. US8323641 B2, 2013. https://doi.org/10.1016/j.(73).
- (11) Devineau, S.; Zargarian, L.; Renault, J. P.; Pin, S. Structure and Function of Adsorbed Hemoglobin on Silica Nanoparticles: Relationship between the Adsorption Process and the Oxygen Binding Properties. *Langmuir* **2017**, *33* (13), 3241–3252. https://doi.org/10.1021/acs.langmuir.6b04281.
- (12) Chan, B. M. C.; Brash, J. L. Adsorption of Fibrinogen on Glass: Reversibility Aspects. *J. Colloid Interface Sci.* **1981**, 82 (1), 217–225. https://doi.org/10.1016/0021-9797(81)90141-7.
- (13) Cox, L. J. Ellipsometry and Polarized Light. *Opt. Acta Int. J. Opt.* **1978**, *25* (3), 270–271. https://doi.org/10.1080/713819761.
- (14) Norde, W.; Anusiem, A. C. I. Adsorption, Desorption

- and Re-Adsorption of Proteins on Solid Surfaces. *Colloids and Surfaces* **1992**, *66* (1), 73–80. https://doi.org/10.1016/0166-6622(92)80122-I.
- (15) Norde, W.; Favier, J. P. Structure of Adsorbed and Desorbed Proteins. *Colloids and Surfaces* 1992, 64 (1), 87–93. https://doi.org/10.1016/0166-6622(92)80164-W.
- (16) Vroman, L.; Lukosevicius, A. Ellipsometer Recordings of Changes in Optical Thickness of Adsorbed Films Associated with Surface Activation of Blood Clotting. Nature 1964, 204 (4959), 701–703. https://doi.org/10.1038/204701b0.
- (17) Rothen, A. The Ellipsometer, an Apparatus to Measure Thickness of Thin Surface Films. *Rev. Sci. Instrum.* 1945, 16 (2), 26–30. https://doi.org/http://dx.doi.org/10.1063/1.177031 5.
- (18) Mrksich, M.; Sigal, G. B.; Whitesides, G. M. Surface Plasmon Resonance Permits in Situ Measurement of Protein Adsorption on Self-Assembled Monolayers of Alkanethiolates on Gold. *Langmuir* 1995, 11 (11), 4383–4385. https://doi.org/10.1021/la00011a034.
- (19) Kößlinger, C.; Uttenthaler, E.; Drost, S.; Aberl, F.; Wolf, H.; Brink, G.; Stanglmaier, A.; Sackmann, E. Comparison of the QCM and the SPR Method for Surface Studies and Immunological Applications. *Sensors Actuators B. Chem.* **1995**, *24* (1–3), 107–112. https://doi.org/10.1016/0925-4005(95)85023-6.
- (20) Caruso, F.; Furlong, D. N.; Kingshott, P. Characterization of Ferritin Adsorption onto Gold. *J. Colloid Interface Sci.* **1997**, *186* (1), 129–140. https://doi.org/10.1006/jcis.1996.4625.
- (21)Höök, F.; Vörös, J.; Rodahl, M.; Kurrat, R.; Böni, P.; Ramsden, J. .; Textor, M.; Spencer, N. .; Tengvall, P.; Gold, J.; Kasemo, B. A Comparative Study of Protein Adsorption on Titanium Oxide Surfaces Using in Situ Ellipsometry, Optical Waveguide Lightmode Spectroscopy, and Quartz Crystal Microbalance/Dissipation. Colloids Surfaces В **Biointerfaces** 2002, 24 155-170. (2), https://doi.org/10.1016/S0927-7765(01)00236-3.
- (22) Höök, F.; Rodahl, M.; Kasemo, B.; Brzezinski, P. Structural Changes in Hemoglobin during Adsorption to Solid Surfaces: Effects of PH, Ionic Strength, and Ligand Binding. *Proc. Natl. Acad. Sci.* 1998, 95 (21), 12271–12276. https://doi.org/10.1073/pnas.95.21.12271.
- (23) Thompson, M.; Arthur, C. L.; Dhaliwal, G. K. Liquid-Phase Piezoelectric and Acoustic Transmission Studies of Interfacial Immunochemistry. *Anal. Chem.* **1986**, *58* (6), 1206–1209. https://doi.org/10.1021/ac00297a051.
- (24) Devineau, S.; Zanotti, J. M.; Loupiac, C.; Zargarian, L.; Neiers, F.; Pin, S.; Renault, J. P. Myoglobin on Silica: A Case Study of the Impact of Adsorption on Protein Structure and Dynamics. *Langmuir* 2013, 29 (44), 13465–13472. https://doi.org/10.1021/la4035479.

- (25) Shen, L.; Zhu, X.-Y. Evidence of a Mobile Precursor State in Nonspecific Protein Adsorption. *Langmuir* **2011**, 27 (11), 7059–7064. https://doi.org/10.1021/la200602v.
- (26) Dominguez-Medina, S.; Kisley, L.; Tauzin, L. J.; Hoggard, A.; Shuang, B.; D. S. Indrasekara, A. S.; Chen, S.; Wang, L. Y.; Derry, P. J.; Liopo, A.; Zubarev, E. R.; Landes, C. F.; Link, S. Adsorption and Unfolding of a Single Protein Triggers Nanoparticle Aggregation. ACS Nano 2016, 10 (2), 2103–2112. https://doi.org/10.1021/acsnano.5b06439.
- (27) Shen, H.; Tauzin, L. J.; Wang, W.; Hoener, B.; Shuang, B.; Kisley, L.; Hoggard, A.; Landes, C. F. Single-Molecule Kinetics of Protein Adsorption on Thin Nylon-6,6 Films. *Anal. Chem.* **2016**, *88* (20), 9926–9933. https://doi.org/10.1021/acs.analchem.5b04081.
- (28) Kastantin, M.; Langdon, B. B.; Chang, E. L.; Schwartz, D. K. Single-Molecule Resolution of Interfacial Fibrinogen Behavior: Effects of Oligomer Populations and Surface Chemistry. J. Am. Chem. Soc. 2011, 133 (13), 4975–4983. https://doi.org/10.1021/ja110663u.
- (29) Mabry, J. N.; Kastantin, M.; Schwartz, D. K. Capturing Conformation-Dependent Molecule-Surface Interactions When Surface Chemistry Is Heterogeneous. ACS Nano 2015, 9 (7), 7237–7247. https://doi.org/10.1021/acsnano.5b02071.
- (30) Weltz, J. S.; Schwartz, D. K.; Kaar, J. L. Surface-Mediated Protein Unfolding as a Search Process for Denaturing Sites. *ACS Nano* **2016**, *10* (1), 730–738. https://doi.org/10.1021/acsnano.5b05787.
- (31) Langdon, B. B.; Kastantin, M.; Schwartz, D. K. Apparent Activation Energies Associated with Protein Dynamics on Hydrophobic and Hydrophilic Surfaces. *Biophys. J.* **2012**, *102* (11), 2625–2633. https://doi.org/10.1016/j.bpj.2012.04.027.
- (32) Mandelbrot, B. B. Stochastic Volatility, Power Laws and Long Memory. *Quant. Financ.* **2001**, *1* (6), 558–559. https://doi.org/10.1080/713665999.
- (33) Bochud, T.; Challet, D. Optimal Approximations of Power Laws with Exponentials: Application to Volatility Models with Long Memory. *Quant. Financ.* **2007**, 7 (6), 585–589. https://doi.org/10.1080/14697680701278291.
- (34) Ripley, B. D. Selecting Amongst Large Classes of Models. In *Methods and Models in Statistics*; Imperial College Press, 2004; pp 155–170. https://doi.org/10.1142/9781860945410_0007.
- (35) Burnham, K. P.; Anderson, D. R. Multimodel Inference: Understanding AIC and BIC in Model Selection. Sociological Methods and Research. November 2004, pp 261–304. https://doi.org/10.1177/0049124104268644.
- (36) Newman, M. E. J. Power Laws, Pareto Distributions and Zipf's Law. *Contemp. Phys.* **2005**, *46* (5), 323–351. https://doi.org/10.1080/00107510500052444.

- (37) Penna, M. J.; Mijajlovic, M.; Biggs, M. J. Molecular-Level Understanding of Protein Adsorption at the Interface between Water and a Strongly Interacting Uncharged Solid Surface. *J. Am. Chem. Soc.* **2014**, *136* (14), 5323–5331. https://doi.org/10.1021/ja411796e.
- (38) Kastantin, M.; Schwartz, D. K. Distinguishing Positional Uncertainty from True Mobility in Single-Molecule Trajectories That Exhibit Multiple Diffusive Modes. *Microsc. Microanal.* **2012**, *18*, 793–797. https://doi.org/10.1017/S1431927602010346.
- (39) Kastantin, M.; Walder, R.; Schwartz, D. K. Identifying Mechanisms of Interfacial Dynamics Using Single-Molecule Tracking. *Langmuir* 2012, 28 (34), 12443– 12456. https://doi.org/10.1021/la3017134.
- (40) Kastantin, M.; Schwartz, D. K. Identifying Multiple Populations from Single-Molecule Lifetime Distributions. *Chemphyschem* **2013**, *14* (2), 374–380. https://doi.org/10.1002/cphc.201200838.
- (41) Kastantin, M.; Langdon, B. B.; Schwartz, D. K. A Bottomup Approach to Understanding Protein Layer Formation at Solid-Liquid Interfaces. *Adv. Colloid Interface Sci.* **2014**, *207* (1), 240–252. https://doi.org/10.1016/j.cis.2013.12.006.
- (42) Köhler, S.; Schmid, F.; Settanni, G. The Internal Dynamics of Fibrinogen and Its Implications for Coagulation and Adsorption. *PLoS Comput. Biol.* **2015**, 11 (9), 1–19. https://doi.org/10.1371/journal.pcbi.1004346.
- (43) Folks, J. L.; Chhikara, R. S. The Inverse Gaussian Distribution and Its Statistical Application-A Review. *J. R. Stat. Soc. Ser. B* **1978**, 40 (3), 263–275. https://doi.org/10.1111/j.2517-6161.1978.tb01039.x.
- (44) Gillespie, D. T. A General Method for Numerically Simulating the Stochastic Time Evolution of Coupled Chemical Reactions. *J. Comput. Phys.* **1976**, *22* (4), 403–434. https://doi.org/10.1016/0021-9991(76)90041-3.
- (45) Ma, G. J.; Ferhan, A. R.; Jackman, J. A.; Cho, N.-J. Conformational Flexibility of Fatty Acid-Free Bovine Serum Albumin Proteins Enables Superior Antifouling Coatings. *Commun. Mater.* 2020, 1 (1), 1–11. https://doi.org/10.1038/s43246-020-0047-9.
- (46) Armstrong, M.; Hess, H.; Tsitkov, S. Statistical Inference in Single Molecule Measurements of Protein Adsorption. In Nanoscale Imaging, Sensing, and Actuation for Biomedical Applications XV; Cartwright, A. N., Nicolau, D. V., Fixler, D., Eds.; SPIE, 2018; Vol. 10506, p 46. https://doi.org/10.1117/12.2290918.
- (47) Steinbach, P. J.; Ionescu, R.; Matthews, C. R. Analysis of Kinetics Using a Hybrid Maximum-Entropy/Nonlinear-Least-Squares Method: Application to Protein Folding. *Biophys. J.* **2002**, *82* (4), 2244–2255. https://doi.org/10.1016/S0006-3495(02)75570-7.
- (48) Raut, V. P.; Agashe, M. A.; Stuart, S. J.; Latour, R. A.

- Molecular Dynamics Simulations of Peptide-Surface Interactions. *Langmuir* **2005**, *21* (4), 1629–1639. https://doi.org/10.1021/la047807f.
- [49] Jung, L. S.; Campbell, C. T. Sticking Probabilities in Adsorption from Liquid Solutions: Alkylthiols on Gold. *Phys. Rev. Lett.* **2000**, *84* (22), 5164–5167. https://doi.org/10.1103/PhysRevLett.84.5164.
- (50) Niemann, M.; Kantz, H.; Barkai, E. Fluctuations of 1/f Noise and the Low-Frequency Cutoff Paradox. Phys. Rev. Lett. 2013, 110 (14), 140603. https://doi.org/10.1103/PhysRevLett.110.140603.
- (51) Brokmann, X.; Hermier, J.-P.; Messin, G.; Desbiolles, P.; Bouchaud, J.-P.; Dahan, M. Statistical Aging and Nonergodicity in the Fluorescence of Single Nanocrystals. *Phys. Rev. Lett.* **2003**, *90* (12), 120601. https://doi.org/10.1103/PhysRevLett.90.120601.
- (52) Regner, B. M.; Vučinić, D.; Domnisoru, C.; Bartol, T. M.; Hetzer, M. W.; Tartakovsky, D. M.; Sejnowski, T. J. Anomalous Diffusion of Single Particles in Cytoplasm. *Biophys. J.* 2013, 104 (8), 1652–1660. https://doi.org/10.1016/j.bpj.2013.01.049.
- (53) Van Tassel, P. R.; Guemouri, L.; Ramsden, J. J.; Tarjus, G.; Viot, P.; Talbot, J. A Particle-Level Model of Irreversible Protein Adsorption with a Postadsorption Transition. J. Colloid Interface Sci. 1998, 207, 317–323. https://doi.org/10.1006/jcis.1998.5781.
- (54) Adamczyk, Z.; Barbasz, J.; Cieśla, M. Mechanisms of Fibrinogen Adsorption at Solid Substrates. *Langmuir* **2011**, *27* (11), 6868–6878. https://doi.org/10.1021/la200798d.
- (55) Rabe, M.; Verdes, D.; Seeger, S. Understanding Protein Adsorption Phenomena at Solid Surfaces. *Adv. Colloid Interface Sci.* **2011**, *162* (1–2), 87–106. https://doi.org/10.1016/j.cis.2010.12.007.
- (56) Siegismund, D.; Schroeter, A.; Schuster, S.; Rettenmayr, M. Quantitative Modeling of Fibrinogen Adsorption on Different Biomaterials. *Cell. Mol. Bioeng.* 2013, 6 (2), 210–219. https://doi.org/10.1007/s12195-012-0266-3.
- (57) Vogler, E. A. Protein Adsorption in Three Dimensions. *Biomaterials* **2012**, *33* (5), 1201–1237. https://doi.org/10.1016/j.biomaterials.2011.10.059.
- (58) Nicholls, A.; Sharp, K. A.; Honig, B. Protein Folding and Association: Insights from the Interfacial and Thermodynamic Properties of Hydrocarbons. *Proteins Struct. Funct. Genet.* 1991, 11 (4), 281–296. https://doi.org/10.1002/prot.340110407.
- (59) Nicolau, D. V.; Paszek, E.; Fulga, F.; Nicolau, D. V. Protein Molecular Surface Mapped at Different Geometrical Resolutions. *PLoS One* 2013, 8 (3), e58896. https://doi.org/10.1371/journal.pone.0058896.
- (60) Van Wagenen, R. A.; Rockhold, S.; Andrade, J. D. Probing Protein Adsorption: Total Internal Reflection Intrinsic Fluorescence. In *Biomaterial: Interfacial*

- Phenomena and Applications; 1982; Vol. 199, pp 351–370. https://doi.org/10.1021/ba-1982-0199.ch023.
- (61) Ramsden, J. J. Experimental Methods for Investigating Protein Adsorption Kinetics at Surfaces. *Q. Rev. Biophys.* **1994**, *27* (1), 41–105. https://doi.org/10.1017/S0033583500002900.
- (62) Hlady, V.; Buijs, J.; Jennissen, H. P. [26] Methods for Studying Protein Adsorption. In *Methods in Enzymology*; 1999; pp 402–429. https://doi.org/10.1016/S0076-6879(99)09028-X.
- (63) Romanowska, J.; Kokh, D. B.; Wade, R. C. When the Label Matters: Adsorption of Labeled and Unlabeled Proteins on Charged Surfaces. *Nano Lett.* **2015**, *15* (11), 7508–7513. https://doi.org/10.1021/acs.nanolett.5b03168.
- (64) Winzen, S.; Koynov, K.; Landfester, K.; Mohr, K. Fluorescence Labels May Significantly Affect the Protein Adsorption on Hydrophilic Nanomaterials. *Colloids Surfaces B Biointerfaces* 2016, 147, 124–128. https://doi.org/10.1016/j.colsurfb.2016.07.057.
- (65) Macritchie, F. Proteins at Interfaces. In *Advances in Protein Chemistry*; 1978; pp 283–326. https://doi.org/10.1016/S0065-3233(08)60577-X.
- (66) Vasina, E. N.; Paszek, E.; Nicolau, Jr, D. V.; Nicolau, D. V. The BAD Project: Data Mining, Database and Prediction of Protein Adsorption on Surfaces. *Lab Chip* 2009, 9 (7), 891–900. https://doi.org/10.1039/B813475H.
- (67) Dér, A. Salts, Interfacial Water and Protein Conformation. *Biotechnol. Biotechnol. Equip.* **2008**, *22* (1), 629–633. https://doi.org/10.1080/13102818.2008.10817524.
- (68) Katira, P.; Agarwal, A.; Hess, H. A Random Sequential Adsorption Model for Protein Adsorption to Surfaces Functionalized with Poly(Ethylene Oxide). *Adv. Mater.* **2009**, *21* (16), 1599–1604. https://doi.org/10.1002/adma.200802057.

Table of Content Figure:

